

# Constraining the Axion Portal with $B \rightarrow K\ell^+\ell^-$

Marat Freytsis,<sup>1,2</sup> Zoltan Ligeti,<sup>2</sup> and Jesse Thaler<sup>1,2</sup>

<sup>1</sup>*Berkeley Center for Theoretical Physics, Department of Physics, University of California, Berkeley, CA 94720*

<sup>2</sup>*Theoretical Physics Group, Lawrence Berkeley National Laboratory, University of California, Berkeley, CA 94720*

We investigate the bounds on axion-like states from flavor-changing neutral current  $b \rightarrow s$  decays, assuming the axion couples to the standard model through mixing with the Higgs sector. Such GeV-scale axions have received renewed attention in connection with observed cosmic ray excesses. We find that existing  $B \rightarrow K\ell^+\ell^-$  data impose stringent bounds on the axion decay constant in the multi-TeV range, relevant for constraining the “axion portal” model of dark matter. Such bounds also constrain light Higgs scenarios in the NMSSM. These bounds can be improved by dedicated searches in  $B$ -factory data and at LHCb.

## I. INTRODUCTION

Motivated by a variety of cosmic ray anomalies [1, 2, 3, 4], a new dark matter paradigm has emerged where TeV-scale dark matter interacts with GeV-scale bosons [5, 6, 7]. In one such scenario — dubbed the “axion portal” [8] — dark matter in the Milky Way halo annihilates into light pseudoscalar “axions”. In order to explain the observed galactic electron/positron excess, the axion,  $a$ , is predicted to have a specific mass and decay constant [8]

$$360 < m_a \lesssim 800 \text{ MeV}, \quad f_a \sim 1 - 3 \text{ TeV}. \quad (1)$$

These axions couple to standard model fermions proportional to their Yukawa couplings, and in this mass range the axion dominantly decays as  $a \rightarrow \mu^+\mu^-$ . Other novel dark matter scenarios involving axion-like states have also been proposed [9, 10, 11, 12, 13], which allow for broader range of axion masses and decay constants.

More generally, light axion-like states appear in variety of new physics scenarios, as they are the ubiquitous prediction of spontaneous Peccei-Quinn (PQ) [14] symmetry breaking. The most famous example is the Weinberg-Wilczek axion invoked to solve the strong  $CP$  problem [15, 16], as well as invisible axion variants [17, 18, 19, 20]. Light pseudoscalar particles appear in any Higgs sector with an approximate PQ symmetry, which often occurs in the minimal or next-to-minimal supersymmetric standard models (MSSM and NMSSM). Models of dynamical supersymmetry breaking typically predict an  $R$ -axion [21], whose couplings can mimic PQ-type axions. There has also been speculation [22] that the HyperCP anomaly [23] might be explained by a light axion. Therefore, searches for light axion-like states have the potential to confirm or exclude a variety of new physics models.

In this paper, we show that flavor-changing neutral current  $b \rightarrow s$  decays place stringent bounds on such models. While the coupling of the axion to fermions is flavor-diagonal, the  $b \rightarrow sa$  decay mediated by a top- $W$  penguin diagram is enhanced by the top Yukawa coupling appearing in the top-axion vertex. To our knowledge, Refs. [24, 25, 26] were the first to consider this decay as a search channel for light pseudoscalars, where the  $a$  field was identified with the  $CP$ -odd Higgs  $A^0$  in a two Higgs doublet model (2HDM). The goal of this paper

is to revive this search channel in models like the axion portal, where there is an  $a$  field which mixes with  $A^0$ .

In the parameter range of interest for the axion portal, the axion decays promptly to  $\mu^+\mu^-$ , and we find that existing  $B \rightarrow K\ell^+\ell^-$  data (for  $\ell = e, \mu$ ) can be used to derive multi-TeV constraints on the axion decay constant  $f_a$ , especially for small values of  $\tan\beta$ . For heavier axion-like states with reduced branching fractions to muons,  $B \rightarrow K\ell^+\ell^-$  can still be used to place a bound, relevant for constraining light Higgs scenarios in the NMSSM [27, 28, 29]. The estimates in this paper are likely improvable by dedicated  $B \rightarrow Ka$  searches at BaBar and Belle, and can be further strengthened at LHCb and a possible super  $B$ -factory. These searches are complementary to  $\Upsilon(nS) \rightarrow \gamma a$  searches recently performed by BaBar [30].

In the next section, we review the axion portal Lagrangian, which is relevant for any DFSZ-type axion [19, 20], and use it to calculate the effective  $b \rightarrow sa$  vertex in Sec. III. We sketch the current experimental situation in Sec. IV and derive corresponding bounds in Sec. V. We conclude in Sec. VI.

## II. REVIEW OF THE AXION PORTAL

If one were only interested in studying the tree-level interactions of new axion-like states, it would be sufficient to introduce a new term in the Lagrangian of the form

$$\delta\mathcal{L}_{\text{int}} = \frac{c_\psi}{f_a} \bar{\psi} \gamma_\mu \gamma_5 \psi \partial_\mu a, \quad (2)$$

where  $f_a$  is the axion decay constant and  $c_\psi$  is the fermion charge under the broken  $U(1)$ . By the equations of motion, such a coupling is proportional to the fermion mass parameter, leading to an effective coupling constant  $c_\psi m_\psi / f_a$ . However, the  $b \rightarrow sa$  process we are interested in occurs via a top- $W$  penguin loop. With only Eq. (2), such a diagram is logarithmically sensitive to the cutoff scale [24], so it is necessary to embed the axion coupling in a complete theory to get a reliable bound on  $f_a$ .

The axion portal [8] is an example of a class of theories where the  $b \rightarrow sa$  amplitude is finite. Like the DFSZ axion, the axion arises from spontaneous PQ-symmetry

breaking in a 2HDM. We show that the  $b \rightarrow sa$  amplitude can be derived from the  $b \rightarrow sA^0$  amplitude, where  $A^0$  is the  $CP$ -odd Higgs boson in a PQ-symmetric 2HDM.

Consider a complex scalar field  $S$  carrying  $U(1)_{\text{PQ}}$  charge that gets a vacuum expectation value  $\langle S \rangle \equiv f_a$ . This spontaneous symmetry breaking leads to a light axion-like state,  $a$ ,

$$S = f_a \exp \left[ \frac{i}{\sqrt{2}f_a} a \right]. \quad (3)$$

The assumption in the axion portal (and for any DFSZ-type axion) is that the only operator that transmits PQ charge from  $S$  to the standard model is

$$\delta\mathcal{L} = \lambda S^n h_u h_d + \text{h.c.}, \quad (4)$$

where  $\lambda$  is a (possibly dimensionful) parameter, and  $n$  is an integer. This coupling forces  $h_u h_d$  to carry non-trivial PQ charge, and we assume that the entire Higgs potential preserves the  $U(1)_{\text{PQ}}$  symmetry to a good approximation. For the PQ-symmetric NMSSM [31]  $n = 1$ , and for the original DFSZ axion [19, 20]  $n = 2$ . Either case can be used in the axion portal model of dark matter.

Since the vevs of  $S$ ,  $h_u$ , and  $h_d$  all break the PQ symmetry, the physical axion will be a linear combination of the phases of all three fields.<sup>1</sup> However, in the  $f_a \gg v_{\text{EW}}$  limit, it is computationally more convenient to work in an ‘‘interaction eigenstate’’ basis, where the axion  $a$  only appears in  $S$ , and the  $CP$ -odd Higgs  $A^0$  only appears in the two Higgs doublets in the form:

$$\begin{aligned} h_u &= \begin{pmatrix} v_u \exp \left[ \frac{i \cot \beta}{\sqrt{2}v_{\text{EW}}} A^0 \right] \\ 0 \end{pmatrix}, \\ h_d &= \begin{pmatrix} 0 \\ v_d \exp \left[ \frac{i \tan \beta}{\sqrt{2}v_{\text{EW}}} A^0 \right] \end{pmatrix}, \end{aligned} \quad (5)$$

where  $\tan \beta \equiv v_u/v_d$ ,

$$v_{\text{EW}} \equiv \sqrt{v_u^2 + v_d^2} \equiv \frac{m_W}{g} \simeq 174 \text{ GeV}, \quad (6)$$

and we have omitted the charged Higgs  $H^\pm$  and the  $CP$ -even Higgses for simplicity. The coefficients appearing in front of  $A^0$  ensure that  $A^0$  is orthogonal to the Goldstone boson eaten by the  $Z$  boson.

This exponential parameterization of  $A^0$  is convenient for our purposes, since PQ symmetry implies that mass terms involving  $a$  and  $A^0$  can only appear in Eq. (4). In this basis, the physical degrees of freedom are given by

$$\begin{aligned} a_{\text{phys.}} &= a \cos \theta - A^0 \sin \theta, \\ A^0_{\text{phys.}} &= a \sin \theta + A^0 \cos \theta, \end{aligned} \quad (7)$$

with

$$\tan \theta \equiv n \frac{v_{\text{EW}}}{f_a} \frac{\sin 2\beta}{2}. \quad (8)$$

At this level, the physical axion is massless.<sup>2</sup> A small mass (beyond the contribution from the QCD anomaly) can be generated by a small explicit violation of the PQ symmetry, but the precise way this happens is irrelevant for our discussion.

The dominant decay mode for the axion depends on its mass,  $m_a$ . The axion decay width to an  $\ell^+ \ell^-$  lepton pair is given by

$$\Gamma(a \rightarrow \ell^+ \ell^-) = n^2 \sin^4 \beta \frac{m_a}{16\pi} \frac{m_\ell^2}{f_a^2} \sqrt{1 - \frac{4m_\ell^2}{m_a^2}}. \quad (9)$$

For  $2m_e < m_a < 2m_\mu$ , the dominant decay is  $a \rightarrow e^+ e^-$ . In this mass range, however, strong bounds already exist from  $K \rightarrow \pi a$  decays [32, 33]. With the axion decay to fermions being proportional to their mass-squared,  $a \rightarrow \mu^+ \mu^-$  dominates over  $a \rightarrow e^+ e^-$  for  $m_a > 2m_\mu$ . Note that in the mass range given in Eq. (1), the axion decays within the detector as long as  $f_a \lesssim 1000$  TeV.

The axion decay becomes more complicated at higher masses when hadronic decay modes open up. Ref. [8] estimated that the  $a \rightarrow 3\pi$  channel starts to dominate over the  $\mu^+ \mu^-$  channel at  $m_a \simeq 800$  MeV. Hadronic channels dominate the axion decay until  $m_a \gtrsim 2m_\tau$ , when the  $\tau^+ \tau^-$  channel becomes dominant. However, as emphasized recently in [34], throughout the entire mass range  $2m_\mu < m_a < 2m_b$ , the branching ratio to  $\mu^+ \mu^-$  remains significant, and until the  $\tau^+ \tau^-$  threshold, it never drops below  $\mathcal{O}(10^{-2})$ . For  $m_a > 2m_\tau$ , the branching fraction to muons is approximately

$$\text{Br}(a \rightarrow \mu^+ \mu^-) \simeq \frac{m_\mu^2}{m_\tau^2} \simeq 0.003, \quad (10)$$

with the precise value depending on  $\tan \beta$  through  $\Gamma(a \rightarrow c\bar{c})$  and on the neglected phase space factor.

### III. THE EFFECTIVE $b \rightarrow sa$ COUPLING

By assumption, the physical axion state dominantly couples to standard model fields via its mixing with  $A^0$ . Therefore, at one-loop level, the amplitude for  $b \rightarrow sa$  can be derived from

$$\mathcal{M}(b \rightarrow sa) = -\sin \theta \times \mathcal{M}(b \rightarrow sA^0)_{2\text{HDM}}, \quad (11)$$

where ‘‘2HDM’’ refers to a (PQ-symmetric) 2HDM with no  $S$  field. Moreover, since the final state only contains

<sup>1</sup> This also means that the physical axion decay constant will be a function of the three vevs. The difference is negligible when  $f_a \gg v_{\text{EW}}$ , and we will continue to refer to  $f_a$  as the axion decay constant.

<sup>2</sup> For completeness, the physical  $A^0$  mass is given by  $m^2(A^0_{\text{phys.}}) = \lambda (f_a)^n (2/\sin 2\beta)(1 + \tan^2 \theta)$ .

a single axion field, there is no difference in the relevant Feynman rules between the exponential parameterization in Eq. (5) and the standard linear parameterization of  $A^0$  in the two Higgs doublet literature. For concreteness, we will consider a type-II (MSSM-like) 2HDM.<sup>3</sup>

The radiatively induced  $b \rightarrow sA^0$  coupling in a type-II 2HDM was calculated in the early 1980's independently in two papers [25, 26]. The dominant contributions come from penguin diagrams involving a top quark, a  $W$  boson and/or charged Higgs  $H^\pm$  boson, and the  $t\bar{t}A^0$  or  $W^\pm H^\mp A^0$  couplings (and corresponding counterterms). The one-loop  $b \rightarrow sA^0$  amplitude is reproduced to lowest order (in the  $m_{B,A^0} \ll m_{W,t,H}$  limit) by the tree-level matrix element of the effective Hamiltonian [25, 26]<sup>4</sup>

$$\mathcal{H} = \frac{g^3 V_{ts}^* V_{tb}}{128 \pi^2} \frac{m_t^2}{m_W^3} (X_1 \cot \beta + X_2 \cot^3 \beta) \bar{s} \gamma^\mu P_L b \partial_\mu A^0. \quad (12)$$

The functions  $X_1$  and  $X_2$  depend on the charged Higgs boson mass  $m_H$ , and are given by

$$\begin{aligned} X_1 &= 2 + \frac{m_H^2}{m_H^2 - m_t^2} - \frac{3m_W^2}{m_t^2 - m_W^2} \\ &\quad + \frac{3m_W^4(m_H^2 + m_W^2 - 2m_t^2)}{(m_H^2 - m_W^2)(m_t^2 - m_W^2)^2} \ln \frac{m_t^2}{m_W^2} \\ &\quad + \frac{m_H^2}{m_H^2 - m_t^2} \left( \frac{m_H^2}{m_H^2 - m_t^2} - \frac{6m_W^2}{m_H^2 - m_W^2} \right) \ln \frac{m_t^2}{m_H^2}, \\ X_2 &= -\frac{2m_t^2}{m_H^2 - m_t^2} \left( 1 + \frac{m_H^2}{m_H^2 - m_t^2} \ln \frac{m_t^2}{m_H^2} \right). \end{aligned} \quad (13)$$

From this effective Hamiltonian, we can calculate various  $B$  decay rates in the 2HDM. These are summarized in App. A for  $B \rightarrow Ka$ ,  $B \rightarrow K^*a$ , and the inclusive  $B \rightarrow X_s a$  rates. Using Eq. (11), the rates in any of these channels relevant for the axion portal are determined by

$$\Gamma(B \rightarrow Ka) = \sin^2 \theta \times \Gamma(B \rightarrow KA^0)_{2\text{HDM}}. \quad (14)$$

#### IV. EXPERIMENTAL BOUNDS

In the parameter range of interest, the axion has a significant decay rate to leptons and decays promptly on

collider timescales. Thus, the axion would manifest itself as a narrow dilepton peak in  $b \rightarrow s\ell^+\ell^-$  decays.

The  $b \rightarrow sa \rightarrow s\ell^+\ell^-$  process contributes to both inclusive and exclusive  $B \rightarrow X_s\ell^+\ell^-$  decays [35, 36]. These final states receive large long-distance contributions from intermediate  $J/\psi$  and  $\psi'$  resonances decaying to  $\ell^+\ell^-$ , which result in removing the surrounding  $q^2$  ( $\equiv m_{\ell^+\ell^-}^2$ ) regions from the measurements. The so-called low- $q^2$  region ( $q^2 \lesssim 7 - 8 \text{ GeV}^2$ ) can probe axion masses up to  $m_a \sim 2.7 \text{ GeV}$ , while the high- $q^2$  region ( $q^2 \gtrsim 14 \text{ GeV}^2$ ) is above the  $a \rightarrow \tau^+\tau^-$  threshold. In general, one can bound the axion contribution in both these regions.

In the low- $q^2$  region, and especially for  $m_a \lesssim 800 \text{ MeV}$  as in Eq. (1), the exclusive mode  $B \rightarrow K\ell^+\ell^-$  is particularly well-suited to constrain  $b \rightarrow sa$ . This is because  $d\Gamma(B \rightarrow K\ell^+\ell^-)/dq^2$  varies slowly at small  $q^2$ , and  $B \rightarrow K\ell^+\ell^-$  has a smaller rate than  $B \rightarrow K^*\ell^+\ell^-$ , thus it gives us the best bound by simply looking at the measured spectrum. In contrast, the exclusive  $B \rightarrow K^*\ell^+\ell^-$  and the inclusive  $B \rightarrow X_s\ell^+\ell^-$  decay modes receive large enhancements from the electromagnetic penguin operator, whose contribution rises steeply at small  $q^2$ , as  $1/q^2$ . This will complicate looking for a small excess in these modes in this region.

For  $m_a \gtrsim 1 \text{ GeV}$ , we expect that the bounds from  $B \rightarrow K\ell^+\ell^-$  and  $K^*\ell^+\ell^-$  may be comparable (possibly even from  $B \rightarrow X_s\ell^+\ell^-$  if a super  $B$ -factory is constructed), and a dedicated experimental analysis should explore how to set the strongest bound, using the rate predictions in App. A. For the remainder of this paper, we focus on  $B \rightarrow K\ell^+\ell^-$ .

Since  $B \rightarrow Ka$  contributes mostly to the  $K\mu^+\mu^-$  final state, and much less to  $Ke^+e^-$ , to set the best possible bound on  $B \rightarrow Ka$ , one needs the  $B \rightarrow K\mu^+\mu^-$  and  $B \rightarrow Ke^+e^-$  spectra separately. This information does not seem to be available in the published papers [37, 38]. Based on the latest world average,  $\text{Br}(B \rightarrow K\ell^+\ell^-) = (4.5 \pm 0.4) \times 10^{-7}$  [37, 38, 39], and the spectrum in Fig. 1 in Ref. [37], it seems to us that

$$\text{Br}(B \rightarrow Ka) \times \text{Br}(a \rightarrow \mu^+\mu^-) < 10^{-7} \quad (15)$$

is a conservative upper bound for any value of the axion mass satisfying  $m_a < m_B - m_K$ .

As we emphasized, BaBar, Belle, and a possible super  $B$ -factory should be able to set a better bound on a narrow resonance contributing to  $B \rightarrow K^{(*)}\mu^+\mu^-$  but not to  $B \rightarrow K^{(*)}e^+e^-$ . Moreover, LHCb will also be able to search for deviations from the standard model predictions in  $B \rightarrow K^{(*)}\ell^+\ell^-$  with significantly improved sensitivity. While we could not find a recent LHCb study for the  $K\ell^+\ell^-$  mode (only for  $K^*\ell^+\ell^-$ ), the fact that the signal to background ratio at the  $e^+e^-$   $B$ -factories is not worse in  $B \rightarrow K\ell^+\ell^-$  than in  $B \rightarrow K^*\ell^+\ell^-$  suggests that LHCb should be able to carry out a precise measurement [40]. Interestingly, since the  $B \rightarrow Ka$  signal is essentially a delta function in  $q^2$ , the bound in Eq. (15) can be improved as experimental statistics increase by considering smaller and smaller bin sizes, without being

<sup>3</sup> The type-I 2HDM model gives the same  $b \rightarrow sA^0$  amplitude to the order we are working; see Ref. [25].

<sup>4</sup> The results published in these two papers differ, a fact which seems to have gone unnoticed—or at least unremarked upon—in the literature. We have redone the calculations both in the unitary gauge and in the Feynman gauge and agree with the result in Ref. [25]. We also agree with Ref. [26] if we replace in their Eq. (9) the second  $\ln(m_t^2/m_W^2)$  term by  $\ln(m_t^2/m_H^2)$ , most likely indicating a simple typographical error. Several papers in the literature seem to use the result as printed in Ref. [26], which has qualitatively wrong implications. For example, it exhibits decoupling in the  $m_H \rightarrow \infty$  limit and singularities when  $m_H \rightarrow m_t$ , whereas the correct result does not.

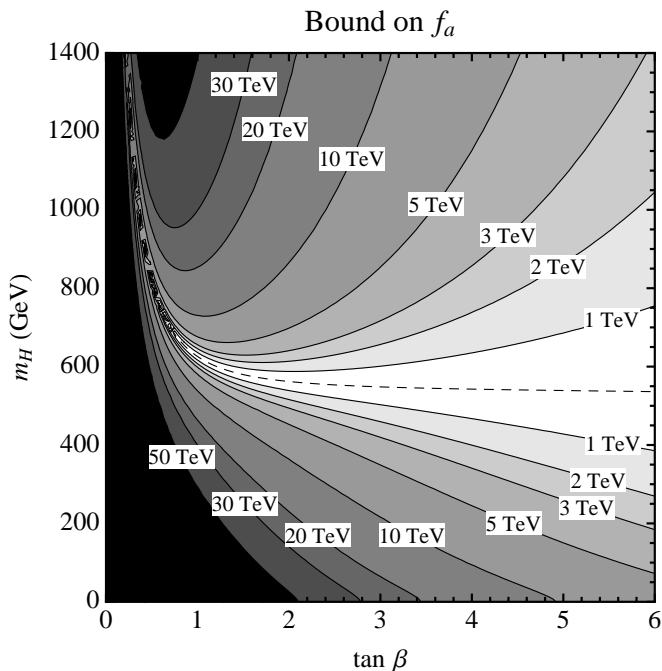


FIG. 1: Bounds on  $f_a$  as a function of  $\tan\beta$  and  $m_H$  for  $n = 1$  in Eq. (8), for  $m_a^2 \ll m_B^2$ . For each displayed value of  $f_a$  there are two contour lines, and the region between them is allowed for  $f_a$  below the shown value. The bound disappears along the dashed curve, and gets generically weaker for larger  $\tan\beta$ .

limited by theoretical uncertainties in form factors [41] (or by nonperturbative contributions [42]). The bound on  $f_a$  will increase compared to the results we obtain in the next section, simply by scaling with the bound on  $1/\sqrt{\text{Br}(B \rightarrow Ka)}$ .

## V. INTERPRETATION

We now derive the bounds on  $f_a$  using the calculated  $B \rightarrow Ka$  branching ratio in Eq. (14) and the experimental bound in Eq. (15). We start with the axion portal scenario with  $\text{Br}(a \rightarrow \mu^+\mu^-) \sim 100\%$  and where  $\sin\theta$  is defined in terms of  $f_a$  by Eq. (8). We will then look at the bound on more general scenarios, including the light Higgs scenario in the NMSSM.

For the axion portal, Fig. 1 shows the constraints on  $f_a$  as a function of the charged Higgs boson mass  $m_H$  and  $\tan\beta$ . For concreteness, we take  $n = 1$ ; other values of  $n$  correspond to a trivial scaling of  $f_a$ . In the mass range in Eq. (1), the dependence on  $m_a$  is negligible for setting a bound. The bound on  $f_a$  is in the multi-TeV range for low values of  $\tan\beta$  and weakens as  $\tan\beta$  increases. At each value of  $\tan\beta$ , there is a value of  $m_H$  for which the  $b \rightarrow sa$  amplitude in Eq. (12) changes signs, indicated by the dashed curve in Fig. 1, along which the bound disappears. Higher order corrections will affect where this cancellation takes place, but away from a very narrow region near this dashed curve, the derived bound is robust.

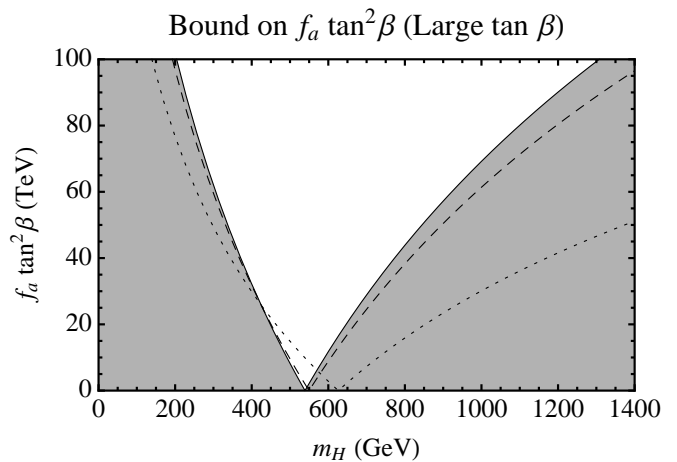


FIG. 2: The shaded regions of  $f_a \tan^2\beta$  are excluded in the large  $\tan\beta$  limit. To indicate the region of validity of the large  $\tan\beta$  approximation, the dashed (dotted) curve shows the bound for  $\tan\beta = 3$  ( $\tan\beta = 1$ ).

As one goes to large values of  $\tan\beta$ , the  $X_1$  piece of Eq. (12) dominates, and  $\sin(2\beta)/2 = 1/\tan\beta + \mathcal{O}(1/\tan^3\beta)$ . In this limit, the constraint takes a particularly simple form that only depends on the combination  $f_a \tan^2\beta$ , as shown in Fig. 2. Except in the region close to  $m_H \sim 550$  GeV, the bound is better than  $f_a \tan^2\beta \gtrsim \text{few} \times 10$  TeV.

These  $B \rightarrow Ka$  bounds are complementary to those recently set by BaBar [30] in  $\Upsilon(nS) \rightarrow \gamma a \rightarrow \gamma \mu^+\mu^-$ :

$$f_a \gtrsim (1.4 \text{ TeV}) \times \sin^2\beta. \quad (16)$$

For example, for  $m_H \simeq 400$  GeV, the  $\Upsilon$  bound dominates for  $\tan\beta \gtrsim 5$ , while  $B \rightarrow Ka$  dominates for  $\tan\beta \lesssim 5$ .

The bounds in Figs. 1 and 2 apply for a generic axion portal model where  $m_H$  and  $\tan\beta$  are free parameters. One would like some sense of what the expected values of  $m_H$  and  $\tan\beta$  might be in a realistic model. Ref. [8] considered a specific scenario based on the PQ-symmetric NMSSM [31]. In that model small  $\tan\beta$  is preferred, since large  $\tan\beta$  requires fine-tuning the Higgs potential. In addition,  $m_H$  is no longer a free parameter and is approximately related to the mass of the lightest  $CP$ -even scalar  $s_0$  via

$$m_H^2 \simeq m_W^2 + \left( \frac{2}{\sin^2 2\beta} \frac{m_{s_0} f_a}{v_{\text{EW}}} \right)^2. \quad (17)$$

In the context of dark matter, Ref. [8] required  $m_{s_0}$  to be  $\mathcal{O}(10 \text{ GeV})$  to achieve a Sommerfeld enhancement. Taking  $m_{s_0} = 10$  GeV and  $f_a = 2$  TeV as a benchmark, the  $B \rightarrow Ka$  bound requires  $2.5 \lesssim \tan\beta \lesssim 3.0$ , corresponding to  $490 \text{ GeV} \lesssim m_H \lesssim 650 \text{ GeV}$ , in the vicinity of the cancellation region. This bound is very sensitive to  $m_{s_0}$ ; for  $m_{s_0} = 20$  GeV and  $f_a = 2$  TeV, the bounds are  $1.5 \lesssim \tan\beta \lesssim 1.7$  and  $550 \text{ GeV} \lesssim m_H \lesssim 610 \text{ GeV}$ . Note that models like [11] have no preferred value of  $m_H$ , can have larger values of  $f_a$ , and do not disfavor large  $\tan\beta$ .

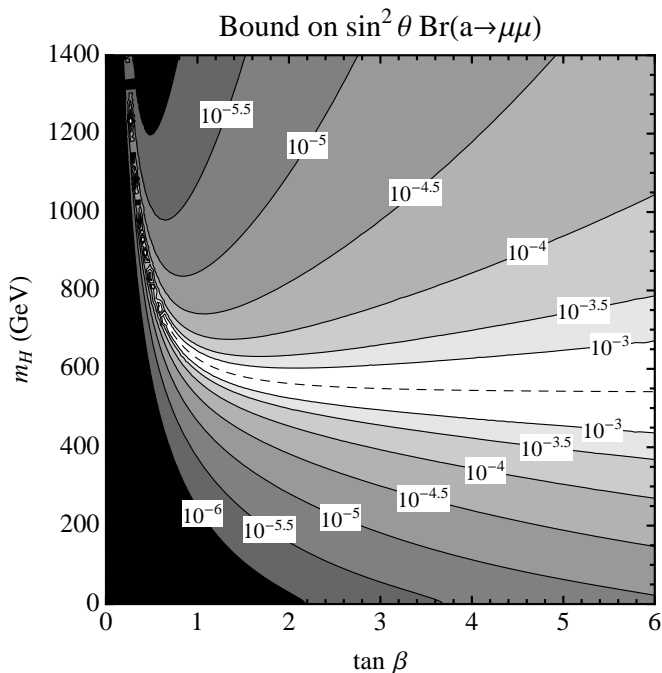


FIG. 3: Bounds on  $\sin^2 \theta \text{Br}(a \rightarrow \mu^+ \mu^-)$  as a function of  $\tan \beta$  and  $m_H$ . Similar to Fig. 1, the successively darker regions going away from the dashed curve are allowed for  $\sin^2 \theta \text{Br}(a \rightarrow \mu^+ \mu^-)$  up to the indicated values. When  $m_a$  is not small compared to  $m_B$ , these bounds should be modified by Eq. (18), but this is a small effect.

As mentioned, these  $B \rightarrow Ka$  constraints apply to any scenario where the branching ratio formula in Eq. (14) applies, i.e. where the axion couplings are determined via Eq. (7), and where  $m_a < m_B - m_K$ . For example, recent studies of light Higgs bosons in the NMSSM [27, 28, 29] and related dark matter constructions [10, 12] also contain a light pseudoscalar whose couplings to standard model fermions can be described in terms of a mixing angle  $\theta$ , as in Eq. (8).<sup>5</sup> There, the mass of the  $a$  field is expected to be  $2m_\tau < m_a < 2m_b$ , with the  $a \rightarrow \mu^+ \mu^-$  branching fraction estimated in Eq. (10).

To show the constraints on such scenarios in a model independent way, we plot the bound on the combination  $\sin^2 \theta \text{Br}(a \rightarrow \mu^+ \mu^-)$  in Fig. 3, in the  $m_a^2 \ll m_B^2$  limit for simplicity. We also show the large  $\tan \beta$  limit in Fig. 4, where the bound is on the combination  $\sin^2 \theta \text{Br}(a \rightarrow \mu^+ \mu^-) / \tan^2 \beta$ . To apply these bounds for the case where  $m_a$  is not small compared to  $m_B$ , one should make the replacement in Figs. 3 and 4 (see App. A),

$$\sin^2 \theta \Rightarrow \sin^2 \theta \frac{\lambda_K(m_a) [f_0(m_a^2)]^2}{(m_B^2 - m_K^2) [f_0(0)]^2} \equiv \sin^2 \theta R(m_a). \quad (18)$$

<sup>5</sup> In the literature,  $\sin \theta$  is often referred to as the “non-singlet fraction”  $\cos \theta_A$  [28].

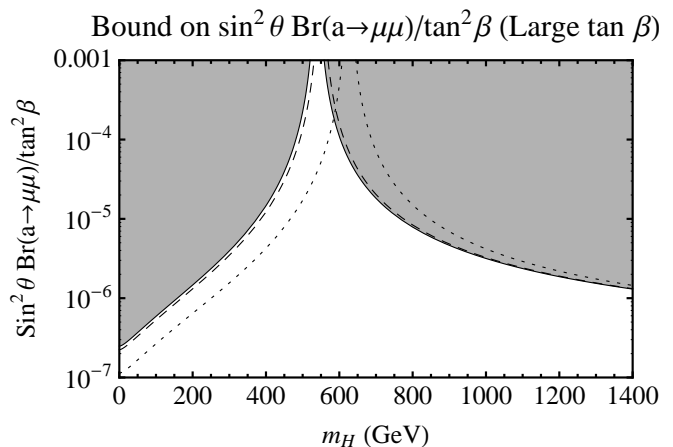


FIG. 4: Bounds on  $\sin^2 \theta \text{Br}(a \rightarrow \mu^+ \mu^-) / \tan^2 \beta$  in the large  $\tan \beta$  limit. The shaded region is excluded, and the dashed (dotted) curve shows  $\tan \beta = 3$  ( $\tan \beta = 1$ ).

Using a simple pole form for the  $q^2$  dependence of  $f_0$  [41], we find that  $R(m_a)$  deviates from unity by less than 20% for  $m_a < 4.6$  GeV (i.e. nearly over the full kinematically allowed region), and so it is a good approximation to neglect  $R(m_a)$ . In the case of NMSSM scenarios, the precise bound depends strongly on the parameters of the theory. To give a sense of the strength of the bound, for  $m_a \sim 4$  GeV,  $m_H \sim 200$  GeV, and using Eq. (10), the bound at large  $\tan \beta$  implies  $\sin^2 \theta / \tan^2 \beta \lesssim 5 \times 10^{-4}$  (and  $\sin^2 \theta \lesssim 2 \times 10^{-4}$  for  $\tan \beta = 1$ ), which is a significant constraint on large mixing angles or small  $\tan \beta$ .

## VI. CONCLUSIONS

In this paper, we explored bounds on axion-like states from flavor-changing neutral current  $b \rightarrow s$  decays. We found that the exclusive  $B \rightarrow K \ell^+ \ell^-$  decay is particularly well-suited to constrain such contributions. In the case of the axion portal (or equivalently, any DFSZ-type axion), we derived a bound from current  $B$ -factory data on the axion decay constant  $f_a$ . The bound is in the multi-TeV range, gets stronger for small  $\tan \beta$ , and depends sensitively on the value of the charged Higgs boson mass. This places tension on the axion portal model of dark matter in the parameter space given in Eq. (1). More generally, there is a constraint on any pseudoscalar with  $2m_\mu < m_a < m_B - m_K$  whose couplings to standard model fermions arise via mixing with the  $CP$ -odd Higgs  $A^0$ . This is true even if  $\text{Br}(a \rightarrow \mu^+ \mu^-) \sim \mathcal{O}(10^{-3})$ , as is the case for light Higgs scenarios in the NMSSM.

We derived our bound using a conservative estimate from the  $q^2$  distribution in  $B \rightarrow K \ell^+ \ell^-$ . The bound could most probably be improved through a dedicated search in existing  $B$ -factory data, and in searches at LHCb and a possible future super  $B$ -factory. The  $B \rightarrow Ka$  search is complementary to axion searches in  $\Upsilon(nS) \rightarrow \gamma a$ , because for fixed mixing angle  $\theta$  in a type-

II 2HDM, the former scales like  $1/\tan^2\beta$  while the latter scales like  $\tan^2\beta$ .

One way to extend our analysis would be to look at axions decaying to hadronic final states. We focused on the decay mode  $a \rightarrow \mu^+\mu^-$ , since the  $a \rightarrow e^+e^-$  mode is already well-constrained by kaon decays, and we were motivated by the parameter space relevant for Ref. [8]. However, as the axion mass increases, other decay channels open up, such as  $a \rightarrow \pi^+\pi^-\pi^0$ ,  $a \rightarrow KK^*$ , etc. These would also be worthwhile to search for in  $B$ -factory data, especially since dark matter models such as [11] are compatible with  $a \rightarrow \pi^+\pi^-\pi^0$  decays. It appears to us that setting bounds in these modes is more complicated than for  $B \rightarrow K\ell^+\ell^-$ , and should be done in dedicated experimental analyses. For constraining higher mass axions, it would be interesting to study whether  $B$ -factories could search for narrow resonances in  $B \rightarrow K\tau^+\tau^-$  at a level of sensitivity no weaker than  $m_\tau^2/m_\mu^2$  times the corresponding bound in  $B \rightarrow K\mu^+\mu^-$ . Combining a number of search channels, one would be able to substantially probe scenarios containing light axion-like states.

**Note Added:** While this paper was being completed, Ref. [43] appeared, which claims much stronger bounds on  $f_a$  than our result. They use a different effective Hamiltonian from Eq. (12), which does not include the effect of charged Higgs bosons, crucial for bounding DFSZ-type axions.

### Acknowledgments

This paper was inspired by a talk by Maxim Pospelov at the SLAC Dark Forces workshop in September 2009. We thank Lawrence Hall and Mark Wise for helpful conversations, and we apologize for making them (temporarily) worried about the correctness of their result. We benefitted from the advice of Mariangela Lisanti, Yasunori Nomura, and Jay Wacker. This work was supported in part by the Director, Office of Science, Office of High Energy Physics of the U.S. Department of Energy under contract DE-AC02-05CH11231.

### APPENDIX A: DECAY RATES

In this appendix, we list the  $B$  decay rates to  $K^{(*)}A^0$  and  $X_s A^0$  in the 2HDM, using the effective Hamiltonian in Eq. (12). These should be combined with Eq. (14) to bound the axion models.

Defining

$$\Gamma_0 = \frac{G_F^3 |V_{ts}^* V_{tb}|^2}{\sqrt{2} 2^{12} \pi^5} m_t^4 m_B^3 (X_1 \cot\beta + X_2 \cot^3\beta)^2, \quad (\text{A1})$$

and

$$\lambda_{K^{(*)}} = \sqrt{(m_B^2 - m_{A^0}^2 - m_{K^{(*)}}^2)^2 - 4m_{A^0}^2 m_{K^{(*)}}^2}, \quad (\text{A2})$$

the  $B \rightarrow KA^0$  decay rate is given by

$$\Gamma(B \rightarrow KA^0) = \Gamma_0 \frac{\lambda_K (m_B^2 - m_K^2)^2}{m_B^6} [f_0(m_{A^0}^2)]^2. \quad (\text{A3})$$

The  $B \rightarrow K^*a$  decay rate is

$$\Gamma(B \rightarrow K^*A^0) = \Gamma_0 \frac{\lambda_{K^*}^3}{m_B^6} [A_0(m_{A^0}^2)]^2. \quad (\text{A4})$$

In both decays we used the standard definitions [35] of the form factors,

$$\begin{aligned} \langle K(p-q) | \bar{s} \not{q} P_L b | B(p) \rangle &= \frac{1}{2} (m_B^2 - m_K^2) f_0(q^2), \quad (\text{A5}) \\ \langle K^*(p-q) | \bar{s} \not{q} P_L b | B(p) \rangle &= -i m_{K^*} (\varepsilon^* \cdot p) A_0(q^2). \end{aligned}$$

(We caution the reader not to confuse  $A^0$  and  $A_0$ , each of which are standard in the respective contexts.)

In Eq. (A1) it is the  $\overline{\text{MS}}$  top quark mass which enters, appropriate both for the coupling to Higgses and in loop integrals. While this distinction is formally a higher order correction, since the rates are proportional to  $m_t^4$ , we use the Tevatron average top mass, converted to  $\overline{\text{MS}}$  at one-loop,  $\overline{m}_t = m_t [1 - 4\alpha_s/(3\pi)] \approx 165$  GeV.

The largest hadronic uncertainty in evaluating the implication of the bound in Eq. (15) is the model dependence in the calculations of the form factor  $f_0(m_a^2)$ , which is an increasing function of  $q^2$ . For  $f_0(0)$ , QCD sum rule calculations obtain values around 0.33, with an order 10% uncertainty [41]. To be conservative, in evaluating the bound on  $f_a$ , we only assume  $f_0(0) > 0.25$  for  $m_a \ll m_B$  (which also covers lower values motivated by SCET-based fits [44]). For  $m_a \gtrsim 2m_\tau$ , relevant for Eq. (18), we use the approximation  $f_0(q^2) = f_0(0)/(1 - q^2/37.5 \text{ GeV}^2)$  [41], which should be good enough for our purposes. For recent QCD sum rule calculations of  $A_0(q^2)$ , relevant for setting a bound using  $B \rightarrow K^*\ell^+\ell^-$ , see Ref. [45].

The inclusive  $B \rightarrow X_s a$  decay rate, which can be calculated (strong interaction) model independently in an operator product expansion, is given at leading order in  $\Lambda_{\text{QCD}}/m_b$  by

$$\Gamma(B \rightarrow X_s A^0) = 2\Gamma_0 \frac{m_b^3}{m_B^3} \left(1 - \frac{m_a^2}{m_b^2}\right). \quad (\text{A6})$$

[1] O. Adriani *et al.* [PAMELA Collaboration], *Nature* **458** (2009) 607 [arXiv:0810.4995 [astro-ph]].

[2] A. A. Abdo *et al.* [The Fermi LAT Collaboration], *Phys.*

- Rev. Lett. **102** (2009) 181101 [arXiv:0905.0025 [astro-ph.HE]].
- [3] F. Aharonian *et al.* [H.E.S.S. Collaboration], Phys. Rev. Lett. **101** (2008) 261104 [arXiv:0811.3894 [astro-ph]].
- [4] F. Aharonian *et al.* [H.E.S.S. Collaboration], arXiv:0905.0105 [astro-ph.HE].
- [5] D. P. Finkbeiner and N. Weiner, Phys. Rev. D **76** (2007) 083519 [arXiv:astro-ph/0702587].
- [6] M. Pospelov, A. Ritz and M. B. Voloshin, Phys. Lett. B **662** (2008) 53 [arXiv:0711.4866 [hep-ph]].
- [7] N. Arkani-Hamed, D. P. Finkbeiner, T. R. Slatyer and N. Weiner, Phys. Rev. D **79** (2009) 015014 [arXiv:0810.0713 [hep-ph]].
- [8] Y. Nomura and J. Thaler, Phys. Rev. D **79** (2009) 075008 [arXiv:0810.5397 [hep-ph]].
- [9] M. Ibe, Y. Nakayama, H. Murayama and T. T. Yanagida, JHEP **0904**, 087 (2009) [arXiv:0902.2914 [hep-ph]].
- [10] Y. Bai, M. Carena and J. Lykken, Phys. Rev. D **80**, 055004 (2009) [arXiv:0905.2964 [hep-ph]].
- [11] J. Mardon, Y. Nomura and J. Thaler, Phys. Rev. D **80** (2009) 035013 [arXiv:0905.3749 [hep-ph]].
- [12] D. Hooper and T. M. P. Tait, Phys. Rev. D **80**, 055028 (2009) [arXiv:0906.0362 [hep-ph]].
- [13] M. Ibe, H. Murayama, S. Shirai and T. T. Yanagida, arXiv:0908.3530 [hep-ph].
- [14] R. D. Peccei and H. R. Quinn, Phys. Rev. Lett. **38** (1977) 1440.
- [15] S. Weinberg, Phys. Rev. Lett. **40** (1978) 223.
- [16] F. Wilczek, Phys. Rev. Lett. **40** (1978) 279.
- [17] J. E. Kim, Phys. Rev. Lett. **43** (1979) 103.
- [18] M. A. Shifman, A. I. Vainshtein and V. I. Zakharov, Nucl. Phys. B **166** (1980) 493.
- [19] M. Dine, W. Fischler and M. Srednicki, Phys. Lett. B **104** (1981) 199.
- [20] A. R. Zhitnitsky, Sov. J. Nucl. Phys. **31** (1980) 260 [Yad. Fiz. **31** (1980) 497].
- [21] A. E. Nelson and N. Seiberg, Nucl. Phys. B **416** (1994) 46 [arXiv:hep-ph/9309299].
- [22] X. G. He, J. Tandean and G. Valencia, Phys. Rev. D **74** (2006) 115015 [arXiv:hep-ph/0610274].
- [23] H. Park *et al.* [HyperCP Collaboration], Phys. Rev. Lett. **94** (2005) 021801 [arXiv:hep-ex/0501014].
- [24] M. B. Wise, Phys. Lett. B **103**, 121 (1981).
- [25] L. J. Hall and M. B. Wise, Nucl. Phys. B **187** (1981) 397.
- [26] J.-M. Frere, J. A. M. Vermaseren and M. B. Gavela, Phys. Lett. B **103** (1981) 129.
- [27] R. Dermisek and J. F. Gunion, Phys. Rev. Lett. **95** (2005) 041801 [arXiv:hep-ph/0502105].
- [28] S. Chang, R. Dermisek, J. F. Gunion and N. Weiner, Ann. Rev. Nucl. Part. Sci. **58**, 75 (2008) [arXiv:0801.4554 [hep-ph]].
- [29] R. Dermisek and J. F. Gunion, Phys. Rev. D **79**, 055014 (2009) [arXiv:0811.3537 [hep-ph]].
- [30] B. Aubert *et al.* [BABAR Collaboration], Phys. Rev. Lett. **103** (2009) 081803 [arXiv:0905.4539 [hep-ex]].
- [31] L. J. Hall and T. Watari, Phys. Rev. D **70** (2004) 115001 [arXiv:hep-ph/0405109].
- [32] V. V. Anisimovsky *et al.* [E949 Collaboration], Phys. Rev. Lett. **93** (2004) 031801 [arXiv:hep-ex/0403036].
- [33] S. S. Adler *et al.* [E787 Collaboration], Phys. Rev. Lett. **88** (2002) 041803 [arXiv:hep-ex/0111091].
- [34] M. Lisanti and J. G. Wacker, Phys. Rev. D **79**, 115006 (2009) [arXiv:0903.1377 [hep-ph]].
- [35] A. Ali, P. Ball, L. T. Handoko and G. Hiller, Phys. Rev. D **61** (2000) 074024, [arXiv:hep-ph/9910221].
- [36] G. Hiller, Phys. Rev. D **70** (2004) 034018 [arXiv:hep-ph/0404220].
- [37] J. T. Wei *et al.* [BELLE Collaboration], Phys. Rev. Lett. **103** (2009) 171801 [arXiv:0904.0770 [hep-ex]]; I. Adachi *et al.* [Belle Collaboration], arXiv:0810.0335 [hep-ex].
- [38] B. Aubert *et al.* [BABAR Collaboration], Phys. Rev. Lett. **102** (2009) 091803 [arXiv:0807.4119 [hep-ex]].
- [39] E. Barberio *et al.* [Heavy Flavor Averaging Group], arXiv:0808.1297 [hep-ex]. and updates at <http://www.slac.stanford.edu/xorg/hfag/>.
- [40] U. Uwer, private communications.
- [41] P. Ball and R. Zwicky, Phys. Rev. D **71** (2005) 014015 [arXiv:hep-ph/0406232].
- [42] M. Bartsch, M. Beylich, G. Buchalla and D. N. Gao, JHEP **0911** (2009) 011 [arXiv:0909.1512 [hep-ph]]; and references therein.
- [43] B. Batell, M. Pospelov and A. Ritz, arXiv:0911.4938 [hep-ph].
- [44] M. C. Arnesen, B. Grinstein, I. Z. Rothstein and I. W. Stewart, Phys. Rev. Lett. **95** (2005) 071802 [arXiv:hep-ph/0504209].
- [45] P. Ball and R. Zwicky, Phys. Rev. D **71** (2005) 014029 [arXiv:hep-ph/0412079].